Design of fuzzy dynamic decoupler for a class of Two-Inputs Two-Outputs nonlinear systems

Szymon Król[*] **and Paweł Dworak**

West Pomeranian University of Technology, Szczecin, Poland

Abstract. This paper deals with the problem of designing a dynamic decoupler for a class of Two-Inputs Two-Outputs nonlinear MIMO systems with experimentally modeled dynamics. The work describes the well-known linear theory of dynamic decoupling of TITO plants and discusses problems related to its application to nonlinear systems. The solution of constructing a fuzzy dynamic decoupler with two possible approaches is proposed. The paper gives a practical example of the synthesis of such a system for the air heater, which is an example of nonlinear thermal plant.

Key words: dynamic decoupling; TITO plant; nonlinear plant; experimental modeling; fuzzy logic

1. INTRODUCTION

Dynamic decoupling of multidimensional Multiple-Inputs, Multiple-Outputs MIMO dynamic plants is a demanding objective in control systems design, studied by many researchers over the past years. Achieving so-called autonomization of the system, ie. eliminating the coupling effects between the inputs and the outputs, is one of the main requirements for the control system and proves to be a challenging task in case of nonlinear plants. In [1] the problem of decoupling the multidimensional nonlinear system was studied, where many linear controllers were derived and adaptive controller structure was discussed. The controllers were designed for different linear models obtained from the linearization of the nonlinear model around adopted operating points of the plant. The possible methods of switching the controllers were proposed in [2], utilizing Takagi-Sugeno fuzzy rules. These studies proved, that the decoupling of nonlinear systems requires such adaptive controller structure, since classical approaches to this task base on linear systems theory. Moreover, for nonlinear systems it is more likely to consider minimizing cross-couplings influences rather than obtaining complete decoupling.

Due to their uncomplicated structure, the very common and widely studied subgroup of Two-Inputs, Two-Outputs TITO multidimensional systems allows for much simpler decoupling techniques, compared to general MIMO decoupling algorithms [3]. It is still an open question how to apply linear decoupling methods to nonlinear TITO systems, whose dynamics have been experimentally identified as a set of linear models and the proposal of such an adaptive system is the main motivation of this paper, in which the fuzzy dynamic decoupler is proposed. The work describes a suitable method for experimental identification of the nonlinear TITO plant as well as the fuzzy decoupler structure with possible intuitive or simplified approach for the design of the fuzzy logic systems. The two methods differs in terms of performance, with the simplified approach being slightly worse. The proposed algorithm and its effectiveness are further illustrated with an application for the

air heater system, which is an example of nonlinear thermal plant. The rest of this paper is organized as follows. Section 2 presents other approaches related to the problem. Section 3 describes the theory of dynamic decoupling of TITO dynamic plants. Section 4 presents the general idea of synthesizing the fuzzy decoupler. Finally, Section 5 gives a practical example of the implementation for the air heater system. Final conclusions are included in Section 6.

2. RELATED WORKS

The possible ways of achieving desired input/output independence were discussed e.g. in [4] with the centralized inverted controllers structure, [5] with the intuitive fuzzy decoupler, [6] with the Elman's neural network, [7] with variable structure Model Following Control or in [8] with the Internal Model Control. Still, the most popular approach is to design a so-called decoupler, ie. linear dynamic compensator of the cross-couplings interferences. This approach includes three possible methods: ideal, simplified and inverted, that were presented e.g. in [9, 10, 11, 12, 13, 14, 15, 16, 17, 18]. The decoupler structure and achieved level of the decoupling depend strictly on the linear model of the plant and its accuracy. Since one deals mostly with the nonlinear systems, such linear model can be derived either from linearization of nonlinear state equations or with experimental modeling in case of more complicated systems, where establishing an acceptable nonlinear model would be too problematic. In such cases the experimental modeling method can be used, which involves obtaining a large amount of experimental data to establish the set of linear models at desired operating points. This approach was profitably used in works [19] for the resistance furnace, [20] for the photo-reactive biological apparatus and [12, 21] for the air heater. Since the decoupler's dynamics is linear, its parameters must change smoothly with the operating point of the plant. Among many ways of switching the coefficients values, the application of fuzzy logic systems seems to be convenient, as they are many possible approaches to their design.

Work [22] presents various ways of developing fuzzy membership functions and rules set, from an intuitive approach,

---
[*]e-mail: Szymon.Krol@zut.edu.pl

based on designer's experience, to an optimal approach to approximate a given data set, e.g. input-output relationship. While an intuitive approach might be suited to the majority of the problems, it is also worth considering an optimal approach for more complex ones. Papers [23, 24, 25] describe the possibility of simultaneous optimization of the membership functions as well as the rules set using well-known Genetic Algorithm (GA) for the purpose of designing a fuzzy controller. The authors encoded fuzzy membership functions and rules set as series of vectors, which formed an individual. The individuals were later compared in the control of a nonlinear dynamic system. The algorithm evolved over time, as each individual had defined time window to perform the control task. However, GA has some disadvantages, namely, it is computationally expensive, especially when dealing with multidimensional optimization problem, such as fuzzy logic system optimization. A better optimization algorithm may be the Imperialist Competitive Algorithm (ICA), inspired by world empires and their rivalries. The basic ICA is presented in paper [26]. In work [27] ICA was compared with GA in terms of optimization of PI controller gains and better results were obtained. Paper [28] introduces Adaptive Differential Mutation variation, which proved its superiority over other ICA variations in solving high-dimensional optimization problems, ie. faster convergence.

The presented bibliography describes many possibilities for dynamic decoupling of TITO dynamic plants. However, the discussed optimization as well as knowledge engineering methods can be profitably used to propose a practical and easy-to-implement method of designing an adaptive fuzzy-logic based dynamic decoupler for nonlinear TITO plants with experimentally modeled dynamics. Moreover, the flexibility of fuzzy logic systems gives the designer two possible approaches, the application of which will be presented in the following Sections of this paper.

3. DYNAMIC DECOUPLING OF TITO DYNAMIC PLANTS

The two-inputs, two-outputs TITO dynamic plant can be described with the following state-space equation

$$\dot{\mathbf{x}}(t) = \mathbf{A}\mathbf{x}(t) + \mathbf{B}\mathbf{u}(t)$$
$$\mathbf{y}(t) = \mathbf{C}\mathbf{x}(t) + \mathbf{D}\mathbf{u}(t), \tag{1}$$

where $\mathbf{A} \in \mathbb{R}^{n \times n}$, $\mathbf{B} \in \mathbb{R}^{n \times 2}$, $\mathbf{C} \in \mathbb{R}^{2 \times n}$, $\mathbf{D} \in \mathbb{R}^{2 \times 2}$ are the state, input, output and feed-trough numerical matrix respectively and $\mathbf{x}(t) \in \mathbb{R}^{n \times 1}$, $\mathbf{u}(t) = [u_1(t) \, u_2(t)]^T$, $\mathbf{y}(t) = [y_1(t) \, y_2(t)]^T$ are state, input and output vector functions respectively. However, in many works [9, 10, 11, 12, 13, 14, 15, 16, 17, 18] the most common representation is the transfer function matrix, resulting from

$$\hat{\mathbf{G}}(s) = \mathbf{C}(s\mathbf{I}_n - \mathbf{A})^{-1}\mathbf{B} + \mathbf{D} = \begin{bmatrix} \hat{g}_{11}(s) & \hat{g}_{12}(s) \\ \hat{g}_{21}(s) & \hat{g}_{22}(s) \end{bmatrix}, \tag{2}$$

where each element is usually a n-th order inertia with dead time

$$\hat{g}_{ij} = \frac{k_{ij}}{\prod_p^n T_{p_{ij}}s + 1} e^{-s\tau_{ij}}, \, i, j = \{1, 2\}. \tag{3}$$
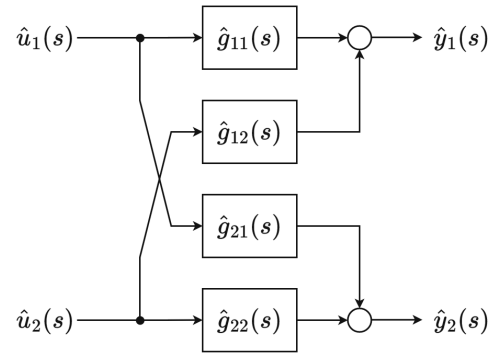

Fig. 1. Block diagram of TITO plant

The block diagram of model from Eq. (2) is presented in Fig. 1. One may instantly notice, that each input influences each output trough cross-coupling dynamics $\hat{g}_{12}(s)$ and $\hat{g}_{21}(s)$. The transforms of the TITO outputs are given as

$$\hat{y}_1(s) = \hat{g}_{11}(s)\hat{u}_1(s) + \hat{g}_{12}(s)\hat{u}_2(s)$$
$$\hat{y}_2(s) = \hat{g}_{21}(s)\hat{u}_1(s) + \hat{g}_{22}(s)\hat{u}_2(s). \tag{4}$$

The main goal of dynamic decoupling is to cancel out $\hat{g}_{12}(s)\hat{u}_2(s)$ and $\hat{g}_{21}(s)\hat{u}_1(s)$ terms in Eq. (4). The most common way of achieving such independence between outputs and inputs is to design a dynamic decoupler $\hat{\mathbf{D}}(s)$, such that

$$\hat{\mathbf{G}}(s)\hat{\mathbf{D}}(s) = \hat{\mathbf{H}}(s) = \begin{bmatrix} \hat{h}_{11}(s) & 0 \\ 0 & \hat{h}_{22}(s) \end{bmatrix}. \tag{5}$$

Note, that the decoupled system $\hat{\mathbf{H}}(s)$ has new input vector $\mathbf{q}(t) = [q_1(t) \, q_2(t)]^T$. By rearranging Eq. (5), the decoupler is given as

$$\hat{\mathbf{D}}(s) = \hat{\mathbf{G}}^{-1}(s)\hat{\mathbf{H}}(s) =$$
$$= \frac{1}{|\hat{\mathbf{G}}(s)|} \begin{bmatrix} \hat{g}_{22}(s)\hat{h}_{11}(s) & -\hat{g}_{12}(s)\hat{h}_{22}(s) \\ -\hat{g}_{21}(s)\hat{h}_{11}(s) & \hat{g}_{11}(s)\hat{h}_{22}(s) \end{bmatrix} =$$
$$= \begin{bmatrix} \hat{d}_{11}(s) & \hat{d}_{12}(s) \\ \hat{d}_{21}(s) & \hat{d}_{22}(s) \end{bmatrix}. \tag{6}$$

Taking into account $\hat{h}_{11}(s) = \hat{g}_{11}(s)$ and $\hat{h}_{22}(s) = \hat{g}_{22}(s)$ yields the ideal decoupler formula

$$\hat{\mathbf{D}}(s) = \begin{bmatrix} \frac{\hat{g}_{11}(s)\hat{g}_{22}(s)}{\hat{g}_{11}(s)\hat{g}_{22}(s) - \hat{g}_{12}(s)\hat{g}_{21}(s)} & -\frac{\hat{g}_{12}(s)\hat{g}_{22}(s)}{\hat{g}_{11}(s)\hat{g}_{22}(s) - \hat{g}_{12}(s)\hat{g}_{21}(s)} \\ -\frac{\hat{g}_{11}(s)\hat{g}_{21}(s)}{\hat{g}_{11}(s)\hat{g}_{22}(s) - \hat{g}_{12}(s)\hat{g}_{21}(s)} & \frac{\hat{g}_{11}(s)\hat{g}_{22}(s)}{\hat{g}_{11}(s)\hat{g}_{22}(s) - \hat{g}_{12}(s)\hat{g}_{21}(s)} \end{bmatrix}. \tag{7}$$

In theory the dynamics of ideally decoupled system matches perfectly the main diagonal dynamics of the plant's model from Eq. (2). However, one may notice high complexity of such solution and particular difficulty in the dead time calculation, therefore the ideal decoupling is rarely used in practice. Moreover, the resulting dynamics of the decoupled system is of little importance in terms of closed-loop control system design. Thus, considering $\hat{d}_{11}(s) = \hat{d}_{22}(s) = 1$ in Eq. (3) results
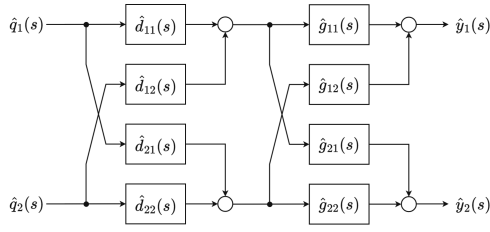
2

Fig. 2. General structure of a decoupled system

in

$$\hat{\mathbf{D}}(s) = \begin{bmatrix} 1 & -\dfrac{\hat{g}_{12}(s)}{\hat{g}_{11}(s)} \\ -\dfrac{\hat{g}_{21}(s)}{\hat{g}_{22}(s)} & 1 \end{bmatrix}, \qquad (8)$$

which is the simplified decoupler formula. To prevent negative dead time values, a solution was proposed in [13] by adopting function $v(\cdot)$, such that

$$v(L) = \max(0, L). \qquad (9)$$

Thus, the decoupler delays are given as

$$\begin{array}{cc} \tau_{d_{11}} = v(\tau_{22} - \tau_{22}) & \tau_{d_{12}} = v(\tau_{12} - \tau_{11}) \\ \tau_{d_{21}} = v(\tau_{21} - \tau_{22}) & \tau_{d_{22}} = v(\tau_{11} - \tau_{12}) \end{array}. \qquad (10)$$

Finally, by inverting simplified decoupler one can establish the inverted decoupler, which combines ideal decoupling effectiveness with the simplicity of simplified decoupler. Figure 2 illustrates the general structure of a decoupled system.

Although the dynamic decoupler design seems indeed to be relatively easy, the problems occur when dealing with nonlinear plants, such as for instance thermal systems. Single linear decoupler will allow for achieving satisfactory results in a single operating point of the decoupled plant, but its performance will decrease in every other unknown region due to the parameters mismatch. Therefore one has to seek for adaptive solution, which will cover the whole state space of the plant.

4. PROPOSED ADAPTIVE FUZZY DYNAMIC DECOUPLER

Consider a nonlinear TITO system with inertial dynamics, that was experimentally modeled at chosen operating points with model from Eq. (2), where each element is a first order plus dead time (FOPDT) transfer function, ie. Eq. (3) for $n = 1$. Because experimental modeling procedure depends strictly on the behavior of the system, it is covered in more details in Section 4. With the identification process a set of coefficients was established, ie. main paths gains k_{11}, k_{22}, time constants T_{11}, T_{22}, delays τ_{11}, τ_{22} as well as cross-couplings gains k_{12}, k_{21}, time constants T_{12}, T_{21} and delays τ_{12}, τ_{21}. As the decoupler itself operates in the open-loop, the adequate values of the coefficients depend on the current values of the new decoupled system inputs $q_1(t)$, $q_2(t)$, ie. each coefficient can be described as a function of inputs

$$c_{ij} = f_{ij}(q_1(t), q_2(t)), \; i, j \in \{1, 2\}, \qquad (11)$$

where c_{ij} stands for one of k_{ij}, T_{ij}, τ_{ij} parameters. Now, for each operating point the dynamic decoupler can be calculated.

For the sake of simplicity, the simplified decoupler from Eq. (8) will be discussed. The decoupler elements are given as

$$\hat{d}_{11}(s) = e^{-\tau_{d_{11}} s}$$

$$\hat{d}_{12}(s) = -\frac{k_{12}(T_{11}s+1)}{k_{11}(T_{12}s+1)} e^{-\tau_{d_{12}} s} = \frac{b_0^{12}s + b_1^{12}}{s + a_{12}} e^{-\tau_{d_{12}} s}$$

$$\hat{d}_{21}(s) = -\frac{k_{21}(T_{22}s+1)}{k_{22}(T_{21}s+1)} e^{-\tau_{d_{21}} s} = \frac{b_0^{21}s + b_1^{21}}{s + a_1^{21}} e^{-\tau_{d_{21}} s}$$

$$\hat{d}_{22}(s) = e^{-\tau_{d_{22}} s}$$

(12)

and can be simply rearranged into state space representation

$$\begin{aligned} \dot{\mathbf{x}}_D(t) &= \mathbf{A}\mathbf{x}_D(t) + \mathbf{B}\mathbf{q}(t) \\ \mathbf{u}(t) &= \mathbf{C}\mathbf{x}_D(t) + \mathbf{D}\mathbf{q}(t), \end{aligned} \qquad (13)$$

where $\mathbf{x}_D(t) = [x_{11}(t)\; x_{12}(t)\; x_{21}(t)\; x_{22}(t)]^T$ is the decoupler state vector, $\mathbf{q}(t) = [q_1(t)\; q_2(t)]^T$ is the decoupled system input vector and $\mathbf{u}_D = [u_1(t)\; u_2(t)]^T$ is the decoupler output vector. The state, input, output and feed-trough matrices are given as

$$\mathbf{A} = \begin{bmatrix} 0 & 0 & 0 & 0 \\ 0 & -a_1^{12} & 0 & 0 \\ 0 & 0 & -a_1^{21} & 0 \\ 0 & 0 & 0 & 0 \end{bmatrix}$$

$$\mathbf{B} = \begin{bmatrix} 0 & 0 \\ 0 & e^{-\tau_{d_{12}} s} \\ e^{-\tau_{d_{21}} s} & 0 \\ 0 & 0 \end{bmatrix}$$

(14)

$$\mathbf{C} = \begin{bmatrix} 0 & b_1^{12} - a_1^{12} b_0^{12} & 0 & 0 \\ 0 & 0 & b_1^{21} - a_1^{21} b_0^{21} & 0 \end{bmatrix}$$

$$\mathbf{D} = \begin{bmatrix} e^{-\tau_{d_{11}} s} & b_0^{12} e^{-\tau_{d_{12}} s} \\ b_0^{21} e^{-\tau_{d_{21}} s} & e^{-\tau_{d_{22}} s} \end{bmatrix},$$

where $e^{-\tau_{d_{ij}}}$ denotes the delay. Note, that the state matrix $\mathbf{A}$ has two unstable poles. However, since $\dot{x}_{11}(t) = \dot{x}_{22}(t) = 0$, the decoupler remains internally stable with two uncontrollable states. To smoothly change the values of decoupler coefficient, ie. approximate the functions from Eq. (11), in the proposed method the fuzzy logic systems were utilized. The matrices $\mathbf{A}, \mathbf{B}, \mathbf{C}, \mathbf{D}$ are constantly changed depending on current input value. The block schematic of the proposed fuzzy decoupler is presented in Fig. 3. The main part of the design concentrates on developing the fuzzy logic system, ie. assigning fuzzy membership functions and fuzzy rules set. In this framework the designer is left with two potential methods, covered in details in the following subsections.
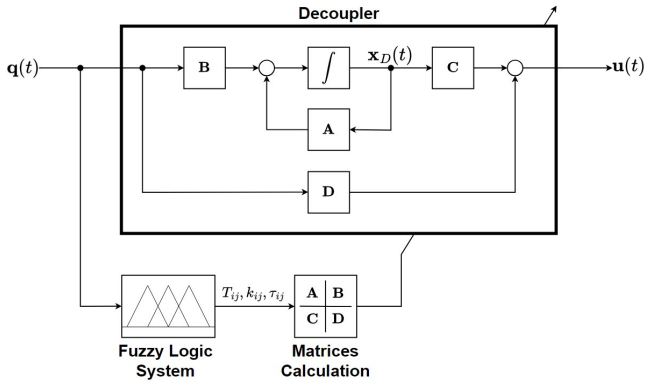
3

Fig. 3. Proposed adaptive fuzzy decoupler, where $\mathbf{A}, \mathbf{B}, \mathbf{C}, \mathbf{D}$ are decoupler's matrices, $T_{ij}, k_{ij}, \tau_{ij}$ are model's parameters and $\mathbf{q}(t), \mathbf{x}_D(t), \mathbf{u}(t)$ are decoupler's input, state and output vectors respectively

Table 1. Part of the set of coefficients

$$\vdots$$

q_1	q_2	c
a_1	b_1	c_1
a_2	b_2	c_2
a_3	b_3	c_3

$$\vdots$$

4.1. The intuitive approach for fuzzy logic systems design

Since the intuitive approach depends on the designer's knowledge and experience, Mamdani type fuzzy systems will be the most appropriate, as this type employs the linguistic rules set. For more convenient implementation, the general Fuzzy System in Fig. 3 can be divided into 8 fuzzy subsystems, each of which is responsible for different coefficient. The number of the subsystems depends on the model adopted in the identification process. Consider the symbolic part of the set of model coefficient c in Table 1. Without loss of generality, the coefficient c can refer to any coefficient in Eq. (12) and the values a_i, b_i are sorted in ascending order. To assign the fuzzy sets, the triangular membership functions will be used. Triangular membership function has three parameters $[s, M, e]$, that define the feet of the fuzzy set and its peak. The membership value of the variable x is given as

$$\mu\left(x \mid [s, M, e]\right) = \max\left(\min\left(\frac{x-s}{M-s}, \frac{e-x}{e-M}\right), 0\right). \quad (15)$$

Now, on the example of input q_1, each input value is assigned to a separate fuzzy set A^i in such a way, that the parameter M is the exact input value a_i, while the parameters s and e have the previous a_{i-1} and next a_{i+1} values respectively. The output fuzzy sets C^i are arranged in the same way. The methodology for constructing both input and output fuzzy sets is illustrated in Fig. 4, where X^i can be either A^i, B^i or C^i, while x_i corresponds to a_i, b_i or c_i respectively. Finally, the fuzzy rules set describes the relationship between inputs and coefficients
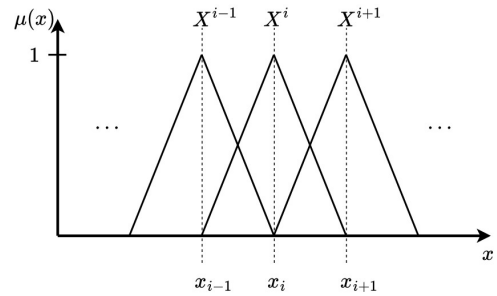

Fig. 4. General idea of assigning intuitive fuzzy sets

values:

$$(1) \text{ IF } q_1 \text{ IS } A^1 \text{ AND } q_2 \text{ IS } B^1 \text{ THEN } c \text{ IS } C^1$$
$$(2) \text{ IF } q_1 \text{ IS } A^2 \text{ AND } q_2 \text{ IS } B^2 \text{ THEN } c \text{ IS } C^2$$
$$(3) \text{ IF } q_1 \text{ IS } A^3 \text{ AND } q_2 \text{ IS } B^3 \text{ THEN } c \text{ IS } C^3$$

$$\vdots$$

Nevertheless, the large experimental data set may result in an excessive number of fuzzy rules and sets. In such cases the simplified approach described in the next subsection may be suitable.

4.2. The simplified approach for fuzzy logic systems design

When the coefficient set is large enough, the intuitive approach for the design may result in an excessive number of fuzzy sets and rules, making the fuzzy logic system over-complicated. Therefore, the fuzzy system can be encoded as a series of vectors, describing the parameters of the membership functions and rules, and optimized. For this purpose, Takagi-Sugeno type is more suitable, as its output is given as a linear combination of the inputs fuzzy sets, ie.:

$$(1) \text{ IF } q_1 \text{ IS } A^i \text{ AND } q_2 \text{ IS } B^j \text{ THEN } c = w_{11}A^i + w_{12}B^j + w_{13}$$

$$\vdots$$

$$(p) \text{ IF } q_1 \text{ IS } A^n \text{ AND } q_2 \text{ IS } B^m \text{ THEN } c = w_{p1}A^n + w_{p2}B^m + w_{p3}$$

To reduce the length of the encoded vectors, ie. the dimension of the searching space, the following Gaussian membership function was selected

$$\mu\left(x \mid [\sigma, M]\right) = e^{-\frac{1}{2}\left(\frac{c-M}{\sigma}\right)^2}, \quad (16)$$

where M and σ define the center and spread. The membership value of the variable. For further simplification it is assumed, that the number of fuzzy sets for both inputs is equal and the
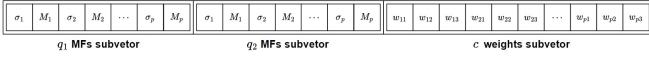
4

Fig. 5. Encoded fuzzy logic system

Fig. 6. Assimilation process

set of rules is fixed and limited to the following form

(1) IF q_1 IS A^1 AND q_2 IS B^1 THEN $c = w_{11}A^1 + w_{12}B^1 + w_{13}$

(2) IF q_1 IS A^2 AND q_2 IS B^2 THEN $c = w_{21}A^2 + w_{22}B^2 + w_{23}$

(3) IF q_1 IS A^3 AND q_2 IS B^3 THEN $c = w_{31}A^3 + w_{32}B^3 + w_{33}$

$$\vdots$$

(p) IF q_1 IS A^p AND q_2 IS B^p THEN $c = w_{p1}A^p + w_{p2}B^p + w_{p3}$.

Thus, the number of fuzzy rules p is equal to the number of input fuzzy sets. Finally, the membership functions parameters and output weights can be represented as a single vector $x \in \mathbf{R}^{1 \times d}$, which forms an individual in the optimization algorithm. The encoding of the fuzzy logic system is illustrated in Fig. 5. In solving optimization problems it is most common to treat M as a relative value, ie.

$$M_i = \sum_{k=1}^{i} M_k, \ i = 1, 2, ..., p. \tag{17}$$

In the selected optimization algorithm, each individual can be evaluated with the following fitness function

$$F_c = \|\mathbf{e}\|_p \tag{18}$$

$$\mathbf{e} = \mathbf{c}_d - \mathbf{c}_{out},$$

where $\mathbf{c}_d$ is the desired coefficient values vector and $\mathbf{c}_{out}$ is the fuzzy system output vector. The norm p depends on the coefficient values and it is recommended to choose 1-norm for fractional values and 2-norm for larger values. Since the fuzzy systems optimization is a high-dimensional problem, one may consider the Imperialist Competitive Algorithm and/or Adaptive Differential Mutation variation of this algorithm described in the next Section.

4.3. Imperialist Competitive Algorithm

Imperialist Competitive Algorithm (ICA) is a stochastic optimization algorithm, inspired by the imperialistic empires in the world and their competition over colonies. It is suitable for high-dimensional optimization problems and is known for its quick convergence [26, 27, 28]. The optimization problem can be formulated as follows

$$\min_{\mathbf{x}_i} F_c(\mathbf{x}_i), \tag{19}$$

where F_c is the cost function and

$$\mathbf{x}_i = [x_{i1}, x_{i2}, ..., x_{id}] \tag{20}$$

is the solution called *country*, bounded to given intervals. The value of the cost function $c_i = F_c(\mathbf{x}_i)$ is the *power* of a country. In the first stage of ICA N countries are randomly generated in the searching space.

Remark 1 *All random numbers in ICA have uniform distribution $U(l_b, u_b)$ in order to increase exploring capabilities*
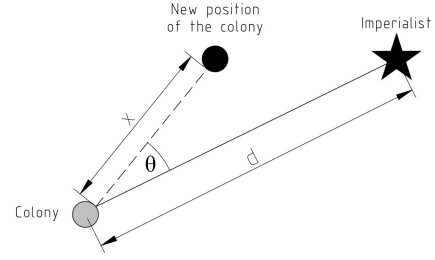
The best N_{imp} countries become the *imperialists*, while the rest N_{col} countries become *colonies*. In the second stage the algorithm determines imperialist normalized power as

$$p_n = \left| \frac{C_n}{\sum_{i=1}^{N_{imp}} C_i} \right| \le 1$$

$$\sum_{p=1}^{N_{imp}} p_n = 1, \tag{21}$$

where $C_n = c_n - \max_i c_i$ and n denotes nth imperialist.

Based on imperialist normalized power, the colonies are randomly divided. Each imperialist posses NC_n colonies, which is calculated as follows

$$NC_n \approx p_n \cdot N_{col}. \tag{22}$$

Divided colonies move toward their imperialist in the process called *assimilation*. In classical ICA variant each colony moves a $\Delta\mathbf{x}_i$ distance along the direction to the imperialist with the deviation angle θ. Both movement values are calculated as

$$\Delta\mathbf{x}_i \sim U(0, \beta \cdot L)$$
$$\Delta\theta \sim U(-\gamma, \gamma), \tag{23}$$

where $\beta > 1$ is the assimilation coefficient, γ is the assimilation angle coefficient and L is the distance between ith colony and its imperialist, given as

$$L = \|\mathbf{x}_n - \mathbf{x}_i\|_2. \tag{24}$$

Final colony position can be denoted as

$$\mathbf{x}_i' = (\mathbf{x}_i + \Delta\mathbf{x}_i) \cdot R \cdot \text{sign}(\mathbf{x}_n - \mathbf{x}_i), \tag{25}$$

where R is the rotation matrix, which depends on the dimension of the searching space. The movement of the colony towards its imperialist is illustrated in Fig. 6. Work [28] introduces new ICA-ADM variant with adaptive differential mutation assimilation strategy, which has proven superiority in solving high-dimensional problems compared to other ICA variants. ICA-ADM calculates mutated colony position as

$$\mathbf{x}_i^m = \mathbf{x}_n + F(\mathbf{x}_{r_1} - \mathbf{x}_{r_2}), \tag{26}$$

where $\mathbf{x}_{r_1}, \mathbf{x}_{r_2}$ are randomly selected colonies from the empire and F is the mutation rate calculated as

$$F = F_u + (F_l - F_l) \frac{F_c(\mathbf{x}_{r_1}) - F_c(\mathbf{x}_n)}{F_c(\mathbf{x}_{r_2}) - F_c(\mathbf{x}_n)}, \tag{27}$$

where F_l and F_u are the lower and upper boundaries of the mutation rate respectively. In order to increase the diversity

5

of the population, the crossover operation is performed. The crossover position $\mathbf{u}_i = [u_{i1}, u_{i2}, ..., u_{id}]$ is established as

$$u_{ij} = \begin{cases} x'_{ij} & \text{if } \psi < CR \\ x_{ij} & \text{if } \psi \geq CR, \end{cases} \tag{28}$$

where $\psi \sim U(0,1)$ and CR is the crossover rate, given as

$$CR = CR_l + (CR_u - CR_l)\frac{F_c(\mathbf{x}_i) - F_c(\mathbf{x}_{worst})}{F_c(\mathbf{x}_n) - F_c(\mathbf{x}_{worst})} \tag{29}$$

Constants CR_l and CR_u denote the lower and upper boundaries of the crossover rate respectively. To maintain good balance between exploration and exploitation both F and CR parameters depend on current iteration. Therefore two indicators I_1, I_2 control when mutation and crossover vary adaptively. When current iteration exceeds one of the indicators, the corresponding parameter has fixed value.

Assimilated colony, which has lower cost function value then the imperialist, becomes new imperialist in the empire, while the old imperialist becomes a colony. During assimilation the revolution process may occur with some determined probability P_{rev}. Revolution means, that a randomly selected colony is replaced with a newly generated one.

After assimilation the empires compete for the weakest colony of the weakest empire or for the collapsing empire. Each empire has an assigned total power

$$TC_n = c_n + \zeta \frac{\sum_{i=1}^{NC_n} c_i}{NC_n}, \tag{30}$$

where $0 < \zeta < 1$ is the cost ratio coefficient. Then the normalized cost of each empire is established as

$$NTC_n = TC_n - \max_i TC_i. \tag{31}$$

Remark 2 *According to Eq. (31), normalized cost of the weakest empire must be equal to zero. Moreover, normalized cost has the most diverse values when comparing empires properties, therefore it is a convenient indicator when searching for the weakest empire*

The possession probability of each empire is defined as

$$P_n = \left| \frac{NTC_n}{\sum_{i=1}^{N_{imp}} NTC_i} \right|, \tag{32}$$

which is analogous to Eq. (21). Possession probabilities form a vector $\mathbf{P}$, from which randomly generated vector $\mathbf{r} \sim U(0,1)$ of the same size is later subtracted. The subtraction forms a new vector $\mathbf{m}$ and the empire with the maximum m_n value wins the competition.

An empire without any colonies collapses, becomes a colony and is divided in the next competition. The algorithm proceeds until the certain number of iterations is completed or until one empire remains.

5. PRACTICAL EXAMPLE

The proposed fuzzy dynamic decoupler was implemented for the air heater system, which is a nonlinear thermal plant. It
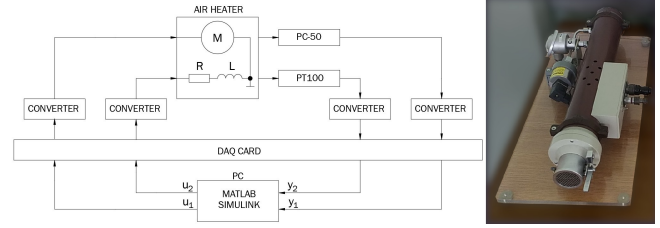

Fig. 7. The air heater system

consists of two inputs $[u_1(t)\ u_2(t)]^T$ to control fan and heating coil respectively. The outputs are the exhaust air pressure $y_1(t)$ and temperature $y_2(t)$. The air heater system is presented in Fig. 7. The current signals are converted to the proportional voltage signals and sampled by the DAQ card, that passes the data to the PC. Control is performed within the Matlab/Simulink Real-Time Workshop environment, where input and output signals are normalised to [0; 1] interval and in such form are presented in the following experiments.

5.1. Experimental modeling

The air heater was experimentally modeled at 32 operating points, as this number was sufficient to obtain satisfactory accuracy. Because temperature changes have no effect on the pressure level, while high pressure cools down the exhaust air, the LTI model adopted at every operating point is given as

$$\mathbf{G}(s) = \begin{bmatrix} \hat{g}_{11}(s) & 0 \\ \hat{g}_{21}(s) & \hat{g}_{22}(s) \end{bmatrix}. \tag{33}$$

To minimize the future size of the fuzzy decoupler, each element in Eq. (33) is assumed to be a FOPDT, where k_{11}, T_{11}, and τ_{11} are the air pressure gain, time constant and delay, k_{22}, T_{22} and τ_{22} are the air temperature gain, time constant and delay and k_{21}, T_{21} and τ_{21} are the cross-coupling gain, time constant and delay. In this example such form is accurate enough to model the dynamics. It turns out, that for such a model both ideal decoupler from Eq. (7) and simplified decoupler from Eq. (8) converge to one simple form

$$\begin{bmatrix} 1 & 0 \\ \hat{d}_{21}(s) & 1 \end{bmatrix}, \tag{34}$$

where

$$\hat{d}_{21}(s) = \frac{\hat{g}_{21}(s)}{\hat{g}_{22}(s)} = \frac{k_{21}T_{22}s + k_{21}}{k_{22}T_{21}s + k_{22}}e^{-v(\tau_{21} - \tau_{22})} \tag{35}$$

and each parameter k_{21}, k_{22}, T_{21}, T_{22}, τ_{21}, τ_{22} changes with the operating point as a function of the input values from Eq. (11). The block diagram of the decoupled model is presented in Fig. 8.

The cross-coupling dynamics $\hat{g}_{21}(s)$ tends to be faster than $\hat{g}_{22}(s)$ temperature dynamics, thus it is possible to assume, that $\tau_{21} \leq \tau_{22}$ in all cases. As a result, the delay in Eq. (35) will always be zero. To further simplify the decoupler structure, the following linear relationship between time constants can be presumed

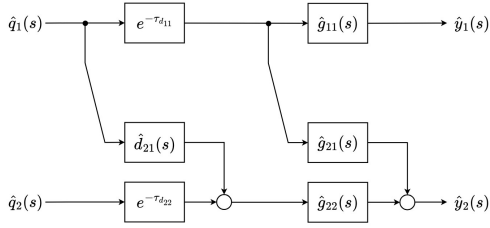$$T_{21} = \alpha T_{22},\ \alpha = 0.95. \tag{36}$$

6

Fig. 8. Block diagram of the decoupled air heater model
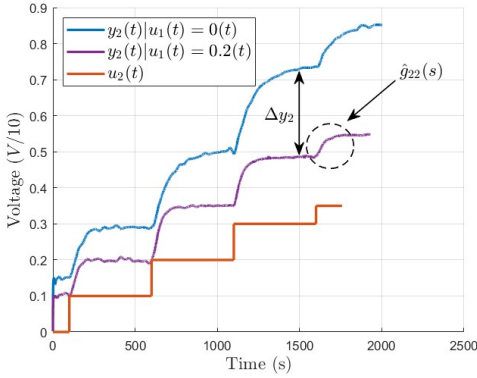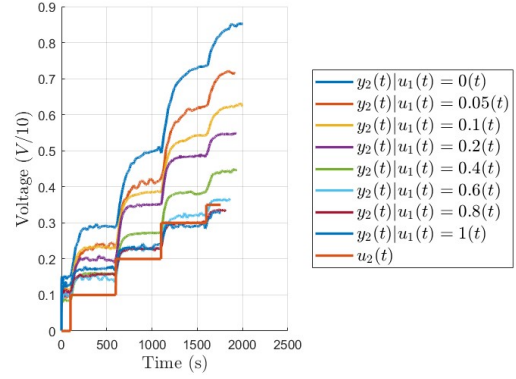

Fig. 9. Identification idea

Fig. 10. Sequences of the identification experiments

Table 2. Adopted constraints of the fuzzy logic systems properties

Parameter	k_{22} FLS	T_{22} FLS	k_{21} FLS
q_1 MFs lower boundaries $[\sigma, M]$	$[10^{-3}, 0]$	$[10^{-3}, 0]$	$[10^{-3}, 0]$
q_1 MFs upper boundaries $[\sigma, M]$	$[0.3, 0.3]$	$[0.3, 0.3]$	$[0.3, 0.3]$
q_2 MFs lower boundaries $[\sigma, M]$	$[10^{-3}, 0]$	$[10^{-3}, 0]$	$[10^{-3}, 0]$
q_2 MFs upper boundaries $[\sigma, M]$	$[0.1, 0.2]$	$[0.1, 0.2]$	$[0.1, 0.2]$
c MFs lower boundaries $[\sigma, M]$	$[10^{-3}, -5]$	$[10^{-3}, 0]$	$[10^{-3}, -5]$
c MFs upper boundaries $[\sigma, M]$	$[1, 5]$	$[20, 100]$	$[1, 5]$
No. MFs	8	12	8

Note, that the described simplifications require some experience with the system and result from a series of experiments, hence, they may not be appropriate in every case. The identification procedure can be divided into following steps:

1. The fan control signal $u_1(t)$ was set to zero. The heating coil control signal $u_2(t)$ was increased step-wise by some value Δu_2 each time the temperature entered the steady state, which resulted in a set of step responses. $u_2(t)$ was increased until the measurement boundary was reached, which took 4 $u_2(t)$ increments. In this step the dynamics $\hat{g}_{22}(s) = \hat{h}_{22}(s)$ of the decoupled system from Eq. (5) was modeled.
2. The fan control signal $u_1(t)$ range was divided into 7 chosen intervals

$$u_1(t) = k(t), \ k \in \{\Delta u_1, 2\Delta u_1, ..., 7\Delta u_1\}. \quad (37)$$

The experiment from Step 1. was repeated for non-zero values of $u_1(t)$.
3. By comparing steady-state values from Step 2. with the desired values from Step 1., the cross-coupling gains can be calculated as

$$k_{21} = \frac{\Delta y_2}{\Delta u_1}. \quad (38)$$

Note, that the choice of Δu_1, Δu_2 and number of intervals is arbitrary and larger number of intervals may result in more accurate model. The idea of the experimental modeling procedure is presented in Fig. 9. With the series of experiments, shown in Fig. 10, the set of experimentally modeled coefficients was created for 32 operating points.

5.2. Fuzzy dynamic decoupler

The decoupler transfer function in Eq. (35) was transformed into the state-space representation as described in Section 3. Every coefficient of the model was approximated by a separate fuzzy logic system. The intuitive fuzzy logic systems were created with the methodology described in Section 3.1. and resulted in 3 fuzzy systems with 7 q_1 sets, 4 q_2 sets, 32 output sets and a set of 32 rules. In the simplified approach, the ICA-ADM ran for $N_{iter} = 500$ iterations. $N_{imp} = 4$ imperialists were chosen from $N = 400$ countries. Mutation rate was bounded to $[F_l = 0.1, F_u = 0.9]$ interval and changed to fixed value $F = 0.5$ after $I_2 = 150$ iterations, while crossover rate was bounded to $[CR_l = 0.1, CR_u = 0.6]$ interval and had fixed value $CR = 0.5$ after $I_1 = 100$ iterations. Revolution probability was set to $P_{rev} = 15\%$. The countries were evaluated with the fitness function from Eq. (18) for $p = 1$. Algorithm stopped after N_{iter} iterations or if only one empire left. The adopted constraints of the fuzzy logic systems properties are listed in Table 2.

5.3. Experimental results

Both intuitive and simplified decouplers were compared with the coupled system in terms of performance. The responses of the systems to the following input signals were recorded

$$q_1(t) = 0.3(t) - 0.2(t - 500) + 0.4(t - 1000) + $$
$$+ 0.15(t - 1500) - 0.45(t - 2000), \quad (39)$$
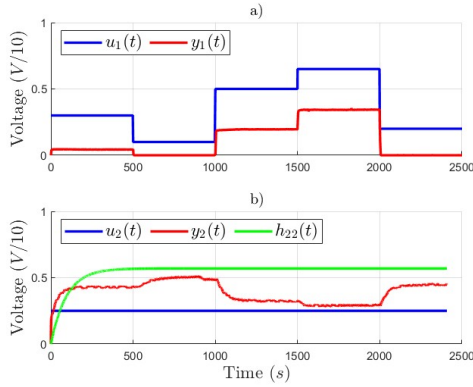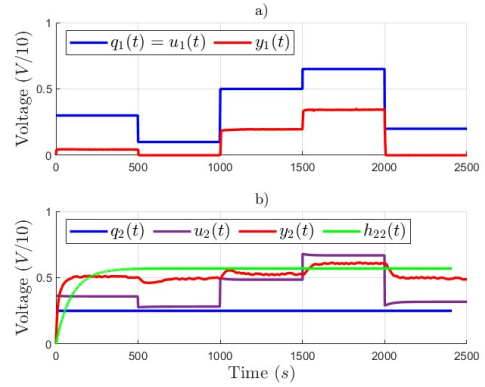$$q_2(t) = \text{const.} = 0.25(t).$$

7

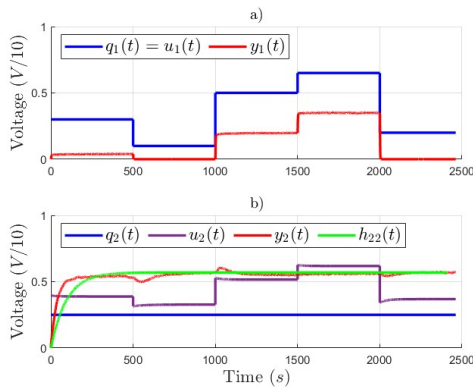**Fig. 11.** Time responses of the coupled system

Fig. 12. Time responses of the decoupled system with intuitive fuzzy systems

It is expected, that the temperature should not change and its dynamics is given as

$$\hat{h}_{22}(s) = \frac{k_{22}}{T_{22}s+1}e^{-\tau_{22}s}. \tag{40}$$

The step response of model from Eq. (40) to the $q_2(t)$ signal in Eq. (39) is given as

$$h_{22}(t) = 0.25k_{22}(1 - e^{-\frac{t-\tau_{22}}{T_{22}}}). \tag{41}$$

It is assumed, that the nominal values of the parameters in Eq. (40) are the averaged output values of intuitive and simplified fuzzy systems for the input values $[q_1 = 0(t) \ q_2 = 0.25(t)]^T$, ie. $k_{22} = 2.2796$, $T_{22} = 94.8403$. The experimental results are presented in Fig. 11. - 13., where **a)** shows the fan input $u_1(t)$, which is equal to the decoupler input $q_1(t)$ (blue), the air pressure $y_1(t)$ (red), while **b)** shows the decoupler input $q_2(t)$ (blue), the decoupler output and heating coil input $u_2(t)$ (purple or blue), the air temperature $y_2(t)$ (red) and the desired temperature dynamics $h_{22}(t)$ (green).

The performance of both coupled and decoupled systems can be evaluated in terms of similarity to the expected temperature changes $h_{22}(t)$ with the following integral criterion

$$J = \int_0^{t_f} |h_{22}(t) - y_2(t)| \, dt. \tag{42}$$

Fig. 13. Time responses of the decoupled system with simplified fuzzy systems

Table 3. Values of the criteria J and I

System	J	I
Coupled	404.0630	35.5%
Decoupled with intuitive FLS	55.5460	11.7%
Decoupled with simplified FLS	151.0528	22.4%

However, the criterion from Eq. (42) does not give a complete understanding of the influence of the cross-coupling. The performance of the decouplers can also be evaluated in terms of achieved invariability of the temperature. The temperature is expected to stay on the level y_2^s, reached in the first steady-state before $t = 500s$. Thus, the second evaluation criterion I can be defined as the maximum deviation from this steady-state for $t > 500s$, expressed as a percentage of the steady-state value y_2^s, ie.

$$I = \frac{\max(|y_2(t) - y_2^s|)}{y_2^s} \, 100\%. \tag{43}$$

The corresponding values of the criteria from Eq. (42) and Eq. (43) are listed in Table 3.

6. CONCLUSIONS

In this paper the structure of fuzzy dynamic decoupler was proposed. The described method is suitable for a class of nonlinear TITO systems with an unknown model, where the experimental modeling is required. The presented method yields two different approaches of designing the fuzzy logic systems, both of which gave some promising results.

The intuitive approach seems to be well-suited for small sets of identification data, but may result in an excessive number of the fuzzy rules and sets. In case of large sets of coefficients, the simplified approach may be more convenient. The use of a ICA-ADM is not necessary, although this algorithm is a proper choice for high-dimensional optimization problems. Simplified fuzzy systems seems to have smoother output surfaces, which is due to the use of Gaussian membership functions.

As shown in the practical example, high performance and significant reduction of the cross-coupling interferences were achieved with the proposed fuzzy dynamic decoupler, with the

8

simplified system being slightly worse, which leaves the properties of the used Takagi-Sugeno systems to be reconsidered. The overall choice of the fuzzy logic system design is, however, a trade-off between accuracy and size of the fuzzy logic system itself. The performance of the fuzzy decoupler can be improved by gathering more identification data in the modeling process, ie. increasing the number of selected operating points, which would result in a more accurate model.

The proposed structure of the fuzzy dynamic decoupler and the described optimization method leave a chance for future development, ie. online optimization of fuzzy systems, which would result in a self-tuning adaptive dynamic decoupler. Such a system may be the subject of future work.

REFERENCES

[1] P. Dworak, "About dynamic decoupling of a nonlinear MIMO dynamic plant," in *2014 19th International Conference on Methods and Models in Automation and Robotics (MMAR)*, 2014, pp. 106–111. [Online]. Available: https://doi.org/10.1109/MMAR.2014.6957333

[2] P. Dworak, "A Type of Fuzzy T-S Controller for a Nonlinear MIMO Dynamic Plant," *Elektronika ir Elektrotechnika*, vol. 20, pp. 8–14, 2014. [Online]. Available: https://doi.org/10.5755/j01.eee.20.5.7091

[3] P. Dworak, "Squaring down plant model and I/O grouping strategies for a dynamic decoupling of left-invertible MIMO plants," *Bulletin of the Polish Academy of Sciences Technical Sciences*, vol. 62, no. 3, pp. 471–479, 2014. [Online]. Available: https://doi.org/10.2478/bpasts-2014-0050

[4] J. Garrido, F. Vázquez, and F. Morilla, "Centralized inverted decoupling for TITO processes," in *2010 IEEE 15th Conference on Emerging Technologies & Factory Automation (ETFA 2010)*, 2010, pp. 1–8. [Online]. Available: https://doi.org/10.1109/ETFA.2010.5641287

[5] M. Hamdy, A. Ramadan, and B. Abozalam, "Comparative study of different decoupling schemes for TITO binary distillation column via PI controller," *IEEE/CAA Journal of Automatica Sinica*, vol. 5, no. 4, pp. 869–877, 2018. [Online]. Available: https://doi.org/10.1109/JAS.2016.7510040

[6] X. Li, Y. Bai, and K. Zhang, "Dynamic Decoupling of the MIMO System Based on the Elman Net," in *2008 International Symposium on Computational Intelligence and Design*, vol. 1, 2008, pp. 537–540. [Online]. Available: https://doi.org/10.1109/ISCID.2008.181

[7] P. Dworak and K. Pietrusewicz, "A variable structure controller for the MIMO thermal plant," *Przegląd Elektrotechniczny*, vol. 86, no. 6, pp. 116–119, 2010.

[8] S. R. Mahapatro, B. Subudhi, S. Ghosh, and P. Dworak, "A comparative study of two decoupling control strategies for a coupled tank system," in *2016 IEEE Region 10 Conference (TENCON)*, 2016. [Online]. Available: https://doi.org/10.1109/TENCON.2016.7848695

[9] M. G. Bulut and F. N. Deniz, "Computation of Stabilizing Decentralized PI Controllers for TITO Systems with Simplified and Inverted Decoupling," in *2020 7th International Conference on Electrical and Electronics Engineering (ICEEE)*, 2020, pp. 294–298. [Online]. Available: https://doi.org/10.1109/ICEEE49618.2020.9102547

[10] V. D. Hajare and B. M. Patre, "Decentralized PID controller for TITO systems using characteristic ratio assignment with an experimental application," *ISA Transactions*, vol. 59, pp. 385–397, 2015. [Online]. Available: https://doi.org/10.1016/j.isatra.2015.10.008

[11] M. Ben Hariz and F. Bouani, "Design of controllers for decoupled TITO systems using different decoupling techniques," in *2015 20th International Conference on Methods and Models in Automation and Robotics (MMAR)*, 2015, pp. 1116–1121. [Online]. Available: https://doi.org/10.1109/MMAR.2015.7284035

[12] S. Król and P. Dworak, "An Application of the Dynamic Decoupling Techniques for a Nonlinear TITO Plant," in *Advanced, Contemporary Control*, M. Pawelczyk, D. Bismor, S. Ogonowski, and J. Kacprzyk, Eds. Cham: Springer Nature Switzerland, 2023, pp. 381–392. [Online]. Available: https://doi.org/10.1007/978-3-031-35170-9_36

[13] Z. Li and Y. Chen, "Ideal, Simplified and Inverted Decoupling of Fractional Order TITO Processes," *IFAC Proceedings Volumes*, vol. 47, no. 3, pp. 2897–2902, 2014, 19th IFAC World Congress. [Online]. Available: https://doi.org/10.3182/20140824-6-ZA-1003.02107

[14] S. K. Lokesh, S. Sharma, and P. K. Padhy, "Study of Different Decoupling Techniques for TITO Time-delay System," in *2021 International Conference on Control, Automation, Power and Signal Processing (CAPS)*, 2021, pp. 1–6. [Online]. Available: https://doi.org/10.1109/CAPS52117.2021.9730644

[15] H. Mokadam, B. Patre, and D. Maghade, "Tuning of multivariable PI/PID controllers for TITO processes using dominant pole placement approach," *Int. J. of Automation and Control*, vol. 7, pp. 21–41, 2013. [Online]. Available: https://doi.org/10.1504/IJAAC.2013.055094

[16] M. Noeding, J. Martensen, N. Lemke, W. Tegethoff, and J. Koehler, "Selection of Decoupling Control Methods Suited for Automated Design for Uncertain TITO Processes," in *2018 IEEE 14th International Conference on Control and Automation (ICCA)*, 2018, pp. 498–505. [Online]. Available: https://doi.org/10.1109/ICCA.2018.8444216

[17] A. Sharma and P. K. Padhy, "Design and implementation of PID controller for the decoupled two input two output control process," in *2017 4th International Conference on Power, Control & Embedded Systems (ICPCES)*, 2017, pp. 1–6. [Online]. Available: https://doi.org/10.1109/ICPCES.2017.8117666

[18] S. Tavakoli, I. Griffin, and P. J. Fleming, "Tuning of decentralised PI (PID) controllers for TITO processes," *Control Engineering Practice*, vol. 14, no. 9, pp. 1069–1080, 2006. [Online]. Available: https://doi.org/10.1016/j.conengprac.2005.06.006

[19] M. Chen, S. Cui, H. Duan, J. Liu, and Y. Liu, "Study on Decoupling Control System of Temperature and pH Concentration in Photoreactive Biological Apparatus," in *2020 IEEE 5th Information Technology and Mechatronics Engineering Conference (ITOEC)*, 2020, pp. 1405–1408. [Online]. Available: https://doi.org/10.1109/ITOEC49072.2020.9141579

[20] Q. Chen, Y. Wang, Z. Xu, X. Chen, T. Zhang, and Y. Zhang, "Modeling, Simulation and Decoupling Control of Resistance Furnace Using MATLAB and Simulink," in *2021 6th International Conference on Automation, Control and Robotics Engineering (CACRE)*, 07 2021, pp. 472–476. [Online]. Available: https://doi.org/10.1109/CACRE52464.2021.9501354

[21] S. Álvarez de Miguel, J. G. Mollocana Lara, C. E. García Cena, M. Romero, J. M. García de María, and J. Gonzaler Aguilar, "Identification model and PI and PID controller design for a novel electric air heater," *Automatika Journal for Control, Measurement, Electronics, Computing and Communications*, vol. 58, no. 1, pp. 55–68, 2017. [Online]. Available: https://doi.org/10.1080/00051144.2017.1342958

[22] T. J. Ross, *Fuzzy Logic with Engineering Applications*. The Atrium, Southern Gate, Chichester, West Sussex PO19 8SQ, England: John Wiley & Sons Ltd, 2004. [Online]. Available: https://doi.org/10.1002/9781119994374

[23] C. Karr and E. Gentry, "Fuzzy control of pH using genetic algorithms," *IEEE Transactions on Fuzzy Systems*, vol. 1, no. 1, pp. 46–, 1993. [Online]. Available: https://doi.org/10.1109/TFUZZ.1993.390283

[24] M. Lee and H. Takagi, "Integrating design stage of fuzzy systems using genetic algorithms," in *[Proceedings 1993] Second IEEE International Conference on Fuzzy Systems*, vol. 1, 1993, pp. 612–617. [Online]. Available: https://doi.org/10.1109/FUZZY.1993.327418

[25] J. Liska and S. Melsheimer, "Complete design of fuzzy logic systems using genetic algorithms," in *Proceedings of 1994 IEEE 3rd International Fuzzy Systems Conference*, vol. 2, 1994, pp. 1377–1382. [Online]. Available: https://doi.org/10.1109/FUZZY.1994.343611

[26] M. Abdollahi, A. Isazadeh, and D. Abdollahi, "Imperialist competitive algorithm for solving systems of nonlinear equations," *Computers & Mathematics with Applications*, vol. 65, no. 12, pp. 1894–1908, 2013. [Online]. Available: https://doi.org/10.1016/j.camwa.2013.04.018

[27] F. Razavi and B. Ghadiri, "Imperialist Competitive Algorithm (ICA)-optimized PI speed control in the Indirect Field-Oriented Control of an IM drive," in *2011 IEEE Colloquium on Humanities, Science and Engineering*, 2011, pp. 445–448. [Online]. Available: https://doi.org/10.1109/CHUSER.2011.6163770

[28] Y. Tang and F. Zhou, "An improved imperialist competition algorithm with adaptive differential mutation assimilation strategy for function optimization," *Expert Systems with Applications*, vol. 211, p. 118686, 2023. [Online]. Available: https://doi.org/10.1016/j.eswa.2022.118686